Cognitive decline and neuroinflammation in a mouse model of obesity: An accelerating role of ageing

Mansi Rajput [a,1], Ihtzaz Ahmed Malik [a,*,1], Aditi Methi [b], Jonathan Alexis Cortés Silva [b,2], Dorothea Fey [a,d], Oliver Wirths [c], André Fischer [b,c,d,e], Jörg Wilting [f], Christine A.F. von Arnim [a,e]

[a] Department of Geriatrics, University Medical Center Goettingen, Robert-Koch-Str. 42, 37075 Goettingen, Germany
[b] German Center for Neurodegenerative Diseases (DZNE), Goettingen, Von-Siebold-Str. 3a, 37075 Goettingen, Germany
[c] Department of Psychiatry, University Medical Center Goettingen, Von-Siebold-Str. 5, 37075 Goettingen, Germany
[d] Cluster of Excellence "Multiscale Bioimaging: from Molecular Machines to Networks of Excitable Cells" (MBExC), University of Göttingen, Germany
[e] German Center for Cardiovascular Research (DZHK), Partner Site Göttingen, 37075 Göttingen, Germany
[f] Institute of Anatomy and Embryology, University Medical Center Goettingen, Kreuzbergring 36, D-37075 Goettingen, Germany

ARTICLE INFO

ABSTRACT

Obesity, a pandemic, worldwide afflicts almost one billion people. Obesity and ageing share several pathological pathways leading to neurological disorders. However, due to a lack of suitable animal models, the long-term effects of obesity on age-related disorders- cognitive impairment and dementia have not yet been thoroughly investigated. Therefore, the current investigation focuses on developing a suitable model to explore the effects of obese-ageing. It also aims to determine whether obesity affects cognitive abilities in an age-dependent manner, and to identify a potential biomarker(s) for cognitive decline.

Cognitive tests were carried out on 6-months and 1-year-old melanocortin-4 receptor (*Mc4r*)-deficient-obese and lean (wildtype) mice. Additionally, brains and sera were harvested for molecular, histological and sero-logical analyses from 6, 12, and 24-months-old mice. Finally, RT-PCR was carried out after hippocampal mRNA sequencing.

The cognitive tests revealed that 1-year-old obese mice have cognitive impairment along with underlying neurodegenerative changes, such as enlarged lateral ventricles. Serum neurofilament light chain (sNfL) levels were also elevated. Lipid accumulation and neuroinflammation were apparent besides, a compromised blood–brain barrier (BBB) indicated by altered junction protein gene expression.

Differentially-expressed genes associated with cognitive decline were identified by mRNA sequencing of hippocampi. One such gene, Secreted Phosphoprotein 1 (Spp1) had markedly increased expression in cognitively-impaired obese mice.

Our findings present an obese-aged mouse model of cognitive decline with neuroinflammation, reduced BBB-integrity and predisposing neurodegenerative changes.

Obese-ageing accelerates the progression of cognitive impairment. Furthermore, Spp1 appears to be a po-tential biomarker for early diagnosis of neuropathological disorders.

1. Introduction

Advancements in medicine have significantly increased human life expectancy. As a result, age-related diseases have become a major socio-economic challenge. Ageing is a complex process resulting in time-dependent losses of physical functions in all organs. Increasing age is

---

a potent risk factor for chronic diseases, including neurodegenerative diseases (NDD) (Scheltens et al., 2016; Gonzales et al., 2022; Hou et al., 2019).

Neurodegeneration is characterized by the irreversible and progressive damage of neurons, eventually leading to cell death (Agrawal, 2020). From an etiological perspective, NDDs such as Alzheimer's disease (AD) are often associated with increasing age (Brown et al., 2005).

The global rise in obesity is contributing to an "obesity epidemic", which accelerates the ageing process and decreases life expectancy (Tam et al., 2020). Obesity-induced metabolic disorders and related inflammation are linked to various health problems, such as dyslipidemia, non-alcoholic fatty liver disease (NAFLD), heart disease, and neurodegenerative diseases (Tam et al., 2020).

In fact, many studies have shown that, in addition to ageing, obesity is one of the most important risk factors for NDDs, including AD (Morys et al., 2023).

Current research, particularly preclinical studies, indicates promising interventions for delaying or even improving chronic diseases through targeted interventions. Thereby, caloric restriction has been highlighted as being important to reduce ageing and age-related health problems by decreasing oxidative stress in humans (Redman et al., 2018).

Moreover, NDD is a group of diseases that exhibit many common and exclusive features. Important common features of all NDDs are neuroinflammation (Chen et al., 2016) and cognitive deficit.

Dysregulation of the immune system and persistent inflammation caused by ageing and obesity are linked to chronic diseases (Frasca et al., 2017). However, the term inflammation is very broad and requires further specification. Neuroinflammation has been shown to correlate with cognitive decline and neurodegenerative diseases. An 'active' immune state has been reported in AD patients (Culpan et al., 2003; Engelhart et al., 2004; Perry et al., 2007; Jonsson et al., 2013), as well as in preclinical investigations (Hong et al., 2016; Leng and Edison, 2021). This aligns with findings that obese individuals are more likely to develop cognitive impairment and neurodegenerative diseases (Albanese et al., 2017; Elena et al., 2022). However, the etiology of this relationship is still not well understood.

Obesity is a complex condition triggered by genetic and environmental factors disrupting energy balance (Tam et al., 2020). Loss-of-function mutations in the melanocortin-4 receptor (*MC4R*) have been reported as the predominant cause of monogenic obesity in humans (Yeo et al., 2003). A clinical study from 2021 found that approximately **7.3%** of the population carries at least one *MC4R* variant from more than 170 distinct variants (Namjou et al., 2021). While, the prevalence in the general population is about **1 in 2,000**, translating roughly to 4 million people worldwide. Similarly, mice in which the *Mc4r* gene (*Mc4r*-null) was specifically disrupted develop an obese phenotype (Huszar et al., 0000). Mc4r is a 7-transmembrane receptor that binds α-melanocyte-stimulating hormone (α-MSH), and is highly expressed in amygdala and the hypothalamus (Kishi et al., 2003). It reduces the feeling of hunger, and also regulates body temperature, sexual appetence, and metabolism (Balthasar et al., 0000). Thereby, *Mc4r* is predominantly expressed in brain and gut (Tao, 2010), but also in liver (Malik et al., 2012). In rodents, a quantitative association between endogenous Mc4r and memory loss was recently described (Zhou et al., 2021).

The development of translational animal models for human disease conditions is a great challenge. For obese-ageing-related cognitive impairment, there are very few rodent models available so far, which may be helpful in deciphering basic mechanisms. The MC4R has highly overlapping functions in men and mice by conveying the feeling of satiety.

There have been very few attempts to understand cognitive functionality in the context of obesity and ageing, and there is a lack of predictive biomarkers for obesity-related NDD.

The aim of our research was to develop a reliable mouse model for obesity that closely resembles the human condition. This model should

allow us to understand whether obesity has an impact on cognitive impairment, and expedites the pathological changes that lead to age-related NDD.

To this end, we conducted the current study using the *Mc4r* knockout mouse model. The *Mc4r*-deficient mouse model accurately recapitulates the human disease in terms of obesity, juvenile diabetes, energy metabolism and neurobiology (Balthasar et al., 0000).

Our data confirm that loss of *Mc4r* is associated with obesity, which accelerates cognitive decline in aged mice, even though weight gain occurs primarily in younger mice. Our transcriptional analyses identify potential genes that may be involved in obese-ageing-induced neuroinflammation and cognitive decline. Thereby, secreted phosphoprotein 1 (*Spp1*, osteopontin) appears to be an early marker and potential trigger for cognitive decline and neuroinflammation, warranting further investigation in humans.

2. Material and Methods

2.1. Experimental animals

C57BL/6J-congenic loxTB *Mc4r* mice along with their corresponding wildtype litter mates were purchased from the Jackson Laboratory, USA. Mice were housed in standard cages on 12h light–dark cycle with food and water *ad libitum*. There were six cohorts of mice: 6-months-old lean and obese, 1-year-old lean and obese, 2-years-old lean and obese as shown in Fig. 1 (a, b, c). All the cohorts were inclusive of male and female mice. Standard protocols approved by the local ethics committee were used during all experiments. All mice studies were reviewed and accepted by the committee of the Central Institute for Animal Experiments of the University Medical Centre Goettingen, and the Lower Saxony State Office for Consumer Protection and Food Safety (No. 33.9–42502-04–20/3346).

6-months and 1-year-old mice cohorts were euthanized post behavioral experiment while 2-years-old were euthanized without experiments by using carbon dioxide (CO_2) asphyxiation. Blood was withdrawn by direct cardiac puncture. Using Micro Sample Tubes with polymer-based gel (Sarstedt™), coagulum of blood was separated from serum upon centrifugation at 15,000 rpm for 15 min. The serum was stored at $-20°C$ for short term and $-80°C$ for long term. Brain tissues along with other organs and blood were isolated from each mouse, thereafter, hippocampal region and cortex of the left-brain hemisphere were micro dissected, cryopreserved with liquid N_2, and stored at $-80°C$ for molecular analyses. The right hemispheres were cryopreserved and stored at $-80°C$ for immunohistochemistry.

2.2. Behavioral tasks

Open field test (OFT) and Morris water-maze test (MWM) were performed as a comprehensive test battery to assess the cognitive and anxiety-like behaviors of the mice in our study. Behavioral tests were performed with 6-months-old and 1-year-old cohorts. However, the 2-years-old cohort was omitted because including these mice could introduce variables (such as sarcopenia (Kerr et al., 2024) and incidence of tumor) related to natural ageing, complicating the interpretation of the results.

2.2.1. Open field test

Each mouse was placed in the center of an acrylic arena with dimensions of 45 x 45 x 40cm for 5 min. The arena is divided into 16 grids. The time spent (s) in the center of the arena (grid 6, 7, 10, and 11) and the total distance covered during the trial was recorded. The chamber/room for the test was sufficiently illuminated for tracking the mouse. After each testing the mice returned to their home cage. The data were recorded using TSE VideoMot2 (TSE Systems) and analyzed with GraphPad Prism 9 software. OFT was performed before and after the completion of water-maze test.
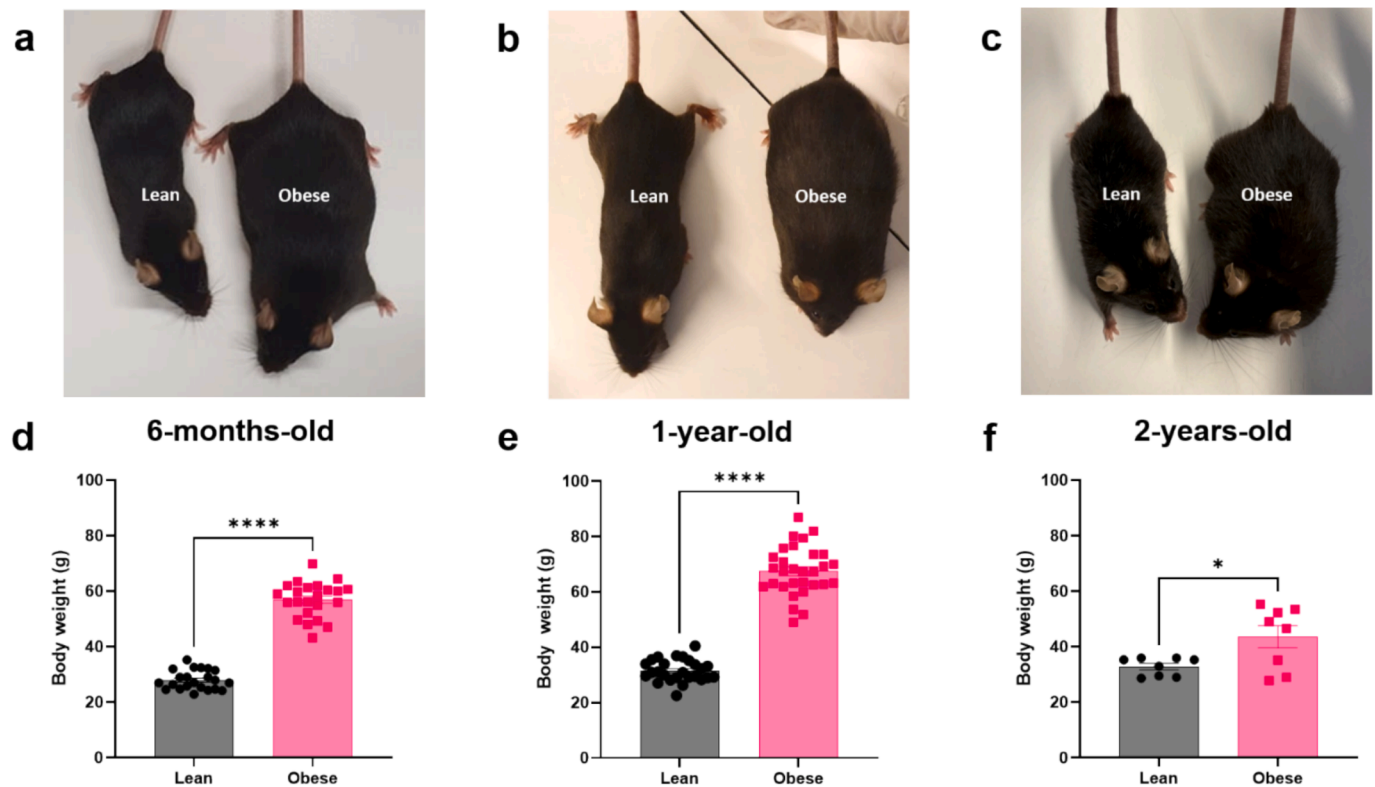
Fig. 1. Mc4r-deficient obese mice. (a-c) Representative images of lean mice and obese mice (C57BL/6J-congenic loxTB Mc4r mice) at the age of 6 months, 1 year, and 2 years (left to right) illustrating the weight gain in obese mice as compared to their lean litter mates. Obese mice started to gain weight by 6 months of age and continued to be heavier through 1 and 2 years of age. (d-f) Graphical representation of body weight associated with Mc4r deficiency in 6-months-old, 1-year-old, and 2-years-old mice. The obese mice were significantly heavier in all age groups. 6-months-old (lean, n = 22; obese, n = 23), 1-year-old (lean, n = 26; obese, n = 30), and 2-years-old (lean, n = 8; obese, n = 8). One-way ANOVA and Welch's *t*-test were applied to the data and represented as mean with SEM.

2.2.2. Morris water maze test

For MWM, the mice were brought into the facility one week before the start of the experiment to allow them to acclimate. The mice were trained in a pool (1.10m in diameter) of water made opaque with nontoxic white paint with an immersed platform (10 x 10 cm). The pool is divided into four quadrants with spatial cues on the sides of the basin serving as landmarks. The standard protocol involves a habituation day (day 0), seven days of training (day 1–7), and test (day 8). The mice go through four trials per training day (60s per trial). Escape latencies, length of path covered, and path to platform were tracked and recorded using TSE VideoMot2 software (TSE Systems). On day 8, the platform was removed following which, speed during the task and quadrant preference were recorded in terms of potential platform crossings (platform quadrant is considered to be the target quadrant). After each testing the mice returned to their home cage.

2.2.3. Spatial strategies and cognitive scores

The strategies used to find the platform during the training days were recorded. For classification of spatial strategies, a modified version of a neural-network algorithm, Morris water maze unbiased strategy classification (MUST-C) was used. It classifies the swimming paths taken by mice into different spatial navigation strategies for every trial in the water maze. Different spatial strategies recorded represent hippocampus-dependent and cognitively demanding strategies along with hippocampus-independent strategies (Illouz et al., 2016; Islam et al., 2021).

Based on the cognitive score system described by Illouz and colleagues (Illouz et al., 2016), cognitive performance score was extended to a score of 10 (Islam et al., 2021). The highest scores are given for hippocampus-dependent strategies like "direct", "corrected", "short chaining" and "focused" to locate the platform, while hippocampus-

independent strategies like "thigmotaxis", "passivity" are scored the least. Weighted cognitive score per day was calculated according to the formula described by Islam and colleagues (Islam et al., 2021).

2.3. Enzyme linked Immunosorbent Assay (ELISA)

2.3.1. Next generation ELISA

Next generation automated sandwich immunoassay was performed in multianalyte cartridges (Bio-techne, Minneapolis, USA) with glass nanoreactor (GNRs) using Ella™ (Bio-techne, Minneapolis, USA). It was performed according to the manufacturer's protocol to identify the neurodegeneration marker neurofilament light chain (NfL, #SPCKB-MP-003168, Bio-techne) and levels of chemokines IFNγ, IL-6, TNFα, CCL2, CXCl10, SDF-1α (#SPCKC-MP-004435, Bio-techne) in sera of mice.

2.3.2. Conventional ELISA

A sandwich ELISA kit (Invitrogen, Cat. #EMSPP1) was used to determine the level of osteopontin (Opn = Spp1) in mouse serum samples. Assays were performed according to the manufacturer's protocol. Serum samples were diluted 50-fold.

2.4. Oil Red O staining

The right hemisphere of brain was isolated and immediately cryopreserved using liquid nitrogen. The cryopreserved brain hemisphere was stored at −80°C for long-term preservation. The brain tissue was trimmed up to a depth of 50μm, 20 times, and then 20–30 serial sections were retrieved. Cryopreserved brain hemispheres were sectioned at a thickness of 10–12 μm using a cryostat (Leica Biosystems). The sections were collected on glass slides and stored at −20°C. The Oil Red O stock solution was prepared by adding 0.5g Oil Red O (Sigma, Cat. #O1391-

500ML) in 100mL of 99% isopropanol. Working solution was made by diluting six parts of stock solution with four parts of distilled water. The working solution was allowed to sit for 24h and then filtered. The frozen slides were washed in distilled water and then incubated in 60% isopropanol for 5 min. The slides were transferred to Oil Red O (filtered) working solution for 10 min followed by a short incubation in isopropanol and water. The slides were then transferred to nuclear stain, hematoxylin for 3–5 min, followed by washing under running tap water for 10 min. Cover-glasses were mounted on the slides with glycerin and were visualized using Plan Fluorite 4X PH and 20X LD PH (BZ-PF04P & BZ-PF20LP) objective lens for bright field imaging in Compact Fluorescence Microscope BZ-X800 (Keyence GmbH, Neu-Isenburg, Germany). At least 2 sections per brain were analyzed.

2.5. Immunofluorescence staining

The brain tissue was isolated, cryopreserved, and sectioned as described above in section 2.4. The sections were mounted onto glass slides and fixed with ice-cold methanol for 9 min followed by chilled acetone for 1 min, and stored at $-20°C$.

The cryo-sections were washed with PBS and then incubated with blocking solution (1X PBS, 1% BSA, and 5% goat serum) for 1h at room temperature. They were then incubated overnight at $4°C$ with primary antibody diluted in PBS. Next day, the slides were washed with PBS and then incubated with appropriate secondary antibody and DAPI diluted in PBS. The slides were washed and then cover-glasses were mounted with a water-based fixative. The slides were analyzed using Plan Fluorite 10X and/or 40X LD PH (BZ-PF10LP, BZ-PF40LP) objective lenses for fluorescence imaging in Compact Fluorescence Microscope BZ-X800 (Keyence GmbH, Neu-Isenburg, Germany). The cell counting was performed using Fiji Image J software (Wisconsin, USA), cell counter plugin. The cells were counted from at least 2 brain slices from each mouse (n=5 per group) with 3 technical replicates. Antibodies are listed in Table 1.

2.6. mRNA sequencing and gene expression profiling

For mRNA sequencing, six independent mice (3 males and 3 females) of each genotype were used, resulting in a significant sample size of n=6 for both lean and obese mice.

Hippocampus was isolated from brain, cryopreserved with liquid nitrogen, and stored at $-80°C$. Total hippocampal RNA was then extracted using the TRIzol method (Life technologies, California, USA) according to the manufacturer's instructions. RNA concentration was quantified by NanoDrop (NanoDrop Technologies, USA). The quality of the RNA samples was assessed with a Fragment Analyzer by Advanced Analytical Technologies before subjecting the RNA samples for library preparation. The libraries were pooled and sequenced using Hiseq4000

(Illumina, Inc, USA). The library type was single-ended with read-lengths of 50bp.

To ensure accurate alignment of all samples, the mRNA sequencing data was aligned and verified. All samples aligned well with each other, and therefore, all were included in the analysis. Sample quality check, mRNA sequencing, and bioinformatical analyses were performed in cooperation with Dr. G. Salinas, NGS Integrative Genomics Core Unit (NIG), Institute of Human Genetics, UMG, Göttingen.

2.7. Pathway enrichment analysis

Gene Ontology overrepresentation analysis was applied to differentially expressed genes using the clusterProfiler R package (version 4.0.0) (Wu et al., 2021;2(3):100141.). FDR cutoff was set to < 0.05.

2.8. Quantitative reverse transcription PCR (qPCR)

For qPCR analyses, total RNA was isolated from hippocampus and cortex of mice using the TRIzol method (Life technologies, California, USA). RNA concentration was measured with NanoDrop (NanoDrop Technologies, USA). cDNA was reverse transcribed from 1μg RNA using the Omniscript® RT Kit (Qiagen, The Netherlands) and XT^{96} thermocycler (VWR International, USA). The reverse transcription-PCR product (cDNA) was diluted to 6.25ng/μl by adding 140μl Ampuwa. Fast green was used for quantification. Signals from target genes were normalized to the house keeping genes Ubiquitin-C or Pecam1. Relative gene expression was analyzed by $2^{-\Delta\Delta CT}$ method (Livak and Schmittgen, 2001). Primers are listed in Table 2.

2.9. Statistical analyses

All the quantitative analyses were carried out on at least five independent animals of each genotype. GraphPad Prism version 9 (Dotmatics, California, USA) was used for all statistical analyses and the generation of graphs. Statistical significance was calculated with Welch's *t*-test and one-way analysis of variance (ANOVA). All experimental errors were calculated as SEM while the data has been represented as mean with SEM. Statistical level of significance was accepted at the conventional critical p-values, *viz*, *$p \leq 0.05$, **$p \leq 0.01$, and ***$p \leq 0.001$ with 95% level of confidence.

3. Results

3.1. C57BL/6J-congenic loxTB Mc4r mice

C57BL/6J-congenic loxTB *Mc4r* mice were generated by insertion of a loxP-flanked transcriptional blocker (TB) upstream of the *Mc4r* ATG site, which serves as an obstacle for the gene promotor to transcribe the gene and eventually disrupts the expression of *Mc4r* (Balthasar et al., 0000). As shown in Fig. 1, these mice phenotypically exhibited severe early-onset obesity along with hyperphagic behaviour (Balthasar et al., 0000), which lasted into old age. Macroscopic images of the mice cohorts at the age of 6 months, 1 year, and 2 years clearly demonstrated

Table 1
List of antibodies used for immunofluorescence staining.

Antibody	Company	Catalog number	Dilution
SPP1 goat pAb	R&D Systems	AF808	1:50
NeuN rabbit mAb	Abclonal	A19086	1:100
CD11b rat mAb	BD Pharmingen	5,502,822	1:50
Synaptotagmin 1 rabbit mAb	Synaptic Systems	105,008	1:500
PSD95 rat mAb	Absolute antibody	1Ab02108-8.4	1:50
Goat-anti-rabbit Alexa Fluor 594	Invitrogen	A11037	1:200
Goat-anti-rat Alexa Fluor 594	Invitrogen	A11055	1:200
Donkey-anti-goat Alexa Fluor 488	Invitrogen	A11055	1:200
Donkey-anti-rabbit Alexa Fluor 594	Invitrogen	A21207	1:200

Table 2
List of primer pairs used in the study.

Primer	Forward	Reverse
Spp1	CTCCTCCCTCCCGGTGAAAG	ATCTGGGTGCAGGCTGTAAA
Hbb-bs	GCCTGAATCACTTGGACAGC	CCCAGCACAATCACGATCAT
Ptgds	GCTCCTTCTGCCCAGTTTTCCT	AGGAGGACCAAACCCATCCAC
Fmod	TAGGCGCTCACTCCTCTCTT	CACTGCATTTTTGTCTCTTGGG
Prg4	TCTCCTTTTTACAGCAAGGGC	CGACAAGCAGACGGGAAGTA
Occludin	GAGGACTGGGTCAGGGAATATC	GACGTCGTCTAGTTCTGCCT
VE-Cadherin	CCTGAGGCAATCAACTGTGC	GGAGGAGCTGATCTTGTCCG
Ubiquitin-C	GCTGGGTAAGCAGGTGGAAGA	TCAGCACAGCCAACTTAACCT
Pecam1	CCCCCAGAACATGGATGTAG	ACACCGTCTCTGTGGCCTC

the obesity phenotype of homozygous knock-out (ko) loxTB *Mc4r* mice (Fig. 1 **a-c**). Fig. 1 **(d-f)** shows a graphical representation of body weights of all mice cohorts. The obese mice weighed significantly more due to their hyperphagic behavior from 6 months through 2 years as compared to their lean counterparts, although at 2 years the difference was smaller but still significant.

3.2. Consequences of obese and healthy ageing on cognitive abilities

Open field test (OFT) offers a measure of exploratory behavior and/ or anxiety. We performed OFT before and after the cognitive test to ensure that anxiety behaviour was not influenced by the handling itself. OFT was performed with 6-months and 1-year-old cohorts (Fig. 2a, Suppl. Fig. 1a). It became obvious that obese mice were less explorative or anxious while the lean C57BL/6J mice showed explorative behavior

common to the mouse strain (Suppl. Fig. 1b; Fig. 2b). This was indicated by a significant difference in time spent in the central zone of the arena. 1-year-old lean mice also travelled significantly longer distance in the arena during exploration as compared to the 1-year-old obese mice (Fig. 2c), whereas 6-months-old lean and obese mice covered almost same distance in the arena (Suppl. Fig. 1c).

To test the effects of obese-ageing on cognition and spatial reference memory, which is typically controlled by the hippocampus, 6-months-old and 1-year-old cohorts were subjected to Morris water-maze test (MWM). MWM assesses the ability of rodents to navigate and locate a submerged platform in a swimming pool, and form a memory during the training days (Morris, 1984). 1-year-old lean mice showed a significant and consistent decrease in escape latency throughout 7 days of training, which was worse in obese mice (Fig. 2e). However, the distance covered to navigate and locate the platform throughout the training days was
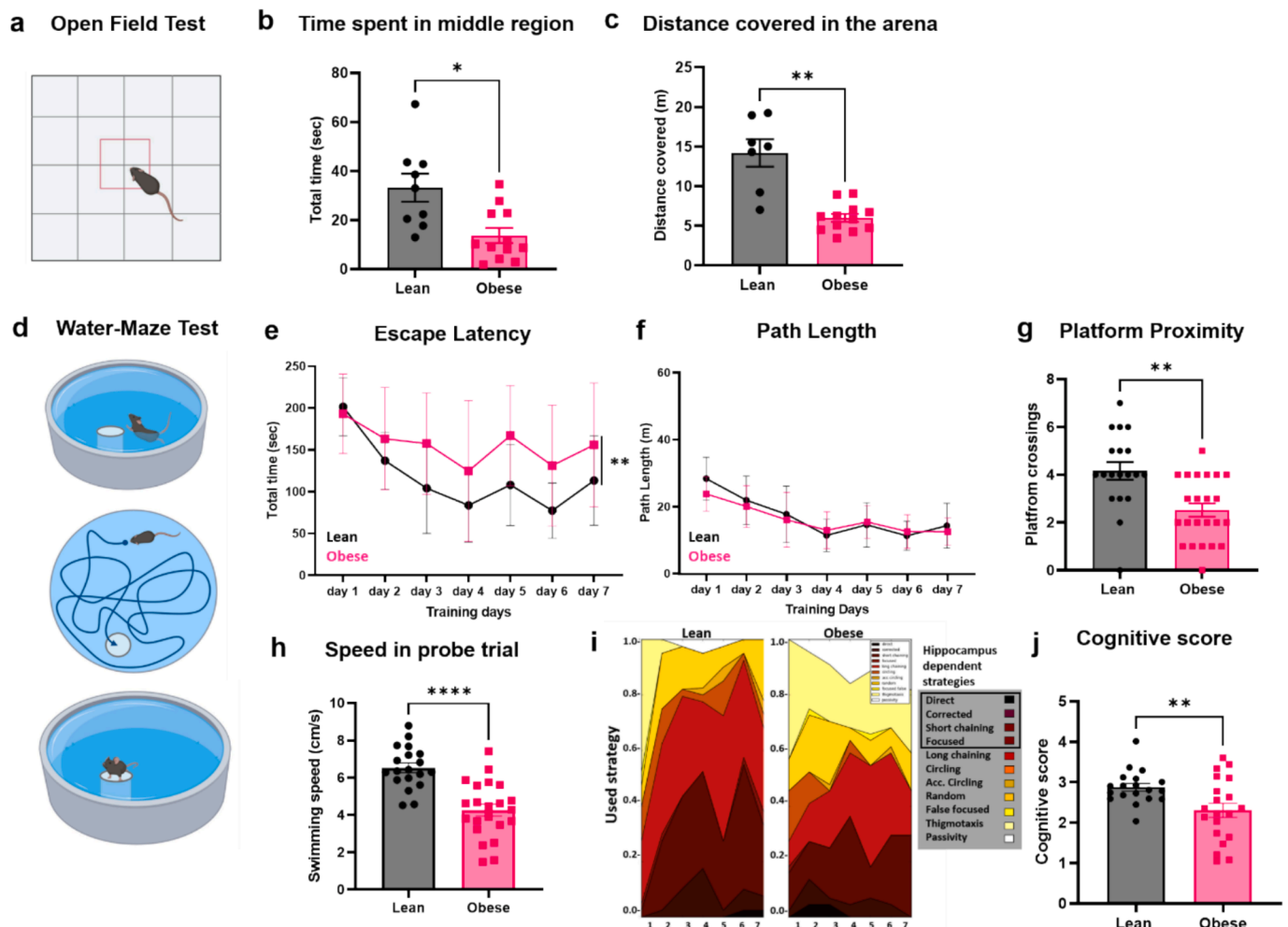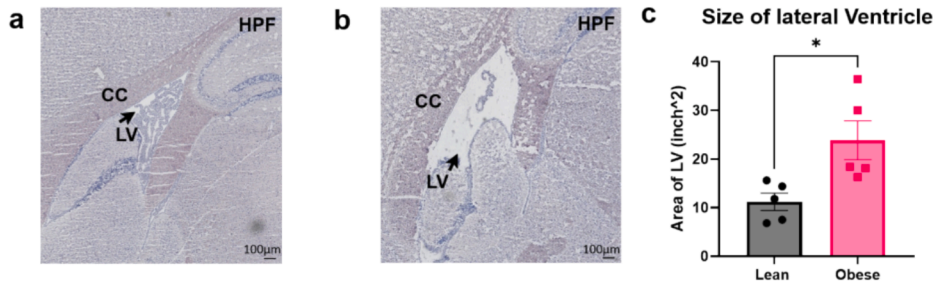

Fig. 2. (a-c) Analyses of activity of 1-year-old lean and obese mice in open field test. Open field test is employed to analyze general locomotion, anxiety, and willingness to explore in lean vs. obese mice. The duration of each trial was 5 min. (a) Schematic representation of Open field test arena. (b) Total time spent by 1-year-old lean and obese mice in the center of the arena. The average time spent in the center by lean mice was significantly more, leading to the interpretation that lean mice were more willing to explore and less anxious. (c) Distance covered by 1-year-old lean mice was significantly more as compared to obese mice. Lean mice, n = 9, obese mice, n = 12. Welch's *t*-test was applied to the data and represented as mean with SEM. **(d − j) Morris Water-maze test in 1-year-old mice.** (d) Schematic representation of water-maze test arena with platform. (e) Escape latency during the water-maze training days comparing 1-year-old lean mice and obese mice. The time taken to find the platform significantly reduced over the training days for both lean and obese mice. Each day, the escape latency of lean mice was significantly lower as compared to obese mice. (f) Path length covered during the water-maze training days. (g) Number of visits to the platform quadrant during the probe test were significantly higher for lean vs. obese mice. (h) Swimming speed during the probe test. (i) Analysis of different strategies used for searching the platform by the two groups. Lean mice notably used more of hippocampus-dependent strategies over the training days indicating better learning and memory as compared to the obese mice. (j) A cognitive score was computed on the basis of scores assigned to hippocampus-dependent strategies used during the training days to navigate toward the platform. The graph indicates that the cognitive abilities of lean mice were significantly better than that of obese mice. Lean mice, n = 19 and obese mice, n = 23. Welch's *t*-test and one-way ANOVA were applied to the data and represented as mean with SEM. While, Brown-Forsythe ANOVA test was applied to data sets shown in (e) and (f) and the graphical representations show mean with SEM. 2a and 2d were created with BioRender.com.
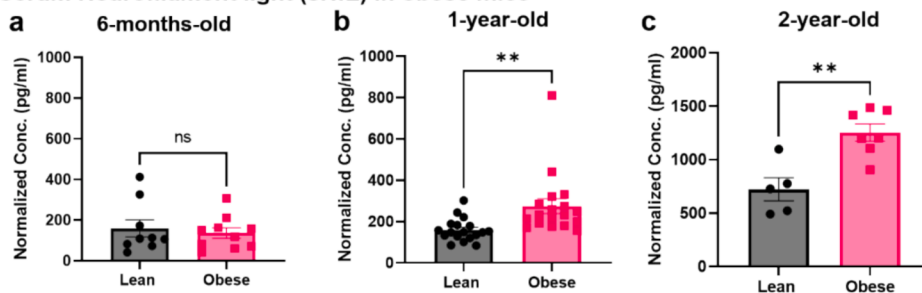
similar for both lean and obese mice as represented in Fig. 2**f**. A probe test was performed after 7 days of training to identify the spatial reference memory of the mice. 1-year-old lean mice showed a significantly higher number of platform crossings during the probe test trial (Fig. 2**g**). Fig. 2**h** demonstrates the swimming speed of the mice during the probe trial. The lean mice swam significantly faster during the trial as compared to the obese mice. For a precise analysis, a modified version of a neural-network algorithm, Morris water maze unbiased strategy classification (MUST-C) was used. Our results showed that most of 1-year-old lean mice showed an increase in usage of hippocampus-dependent

strategies like "direct", "corrected", "short chaining" and "focused" to locate the platform throughout the 7 days of training. This observation suggests intact cognitive function. In contrast, the usage of hippocampus-independent strategies such as "long chaining", "circling", or "thigmotaxis" increased in 1-year-old obese mice indicating impaired cognition (Fig. 2**i**). Eventually, a cognitive score was computed based on MUST-C algorithm. It reflects consistent use of hippocampus-dependent or −independent strategies during the 7 days of training. Behavior-based cognitive scores of 1-year-old lean mice were significantly higher as compared to that of the 1-year-old obese mice (Fig. 2**j**). Morris
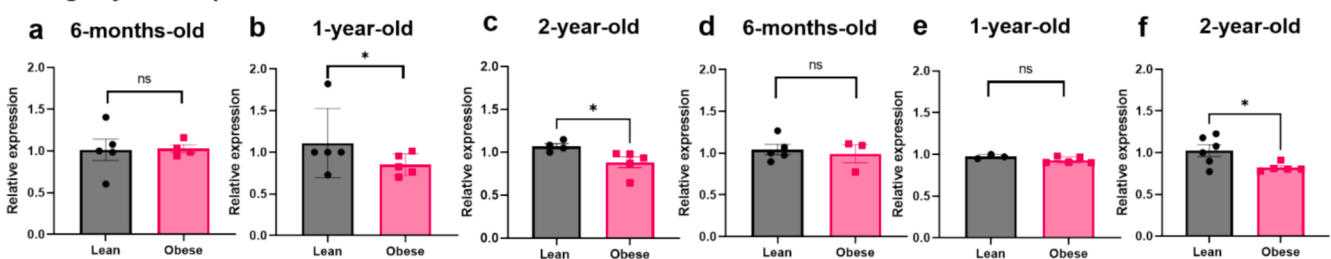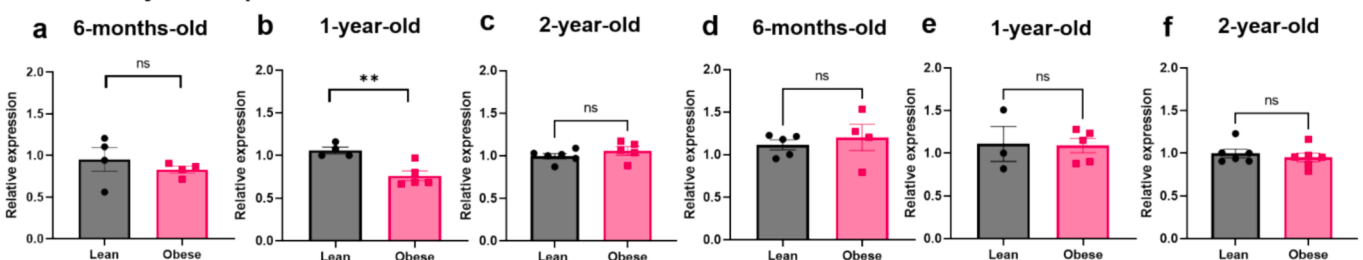

Fig. 3. Hallmarks of neurodegeneration. A (Aa-b) Representative microscopic images **depicting the size of lateral ventricle** in 1-year-old lean mouse brain (left) and obese mouse brain (right). (Ac) Graphical representation of comparison of sizes of lateral ventricles in 1-year-old lean and obese mice. The graph indicates dilation in the lateral ventricles of obese mice brains. Lean mice (n = 5) and obese mice (n = 5). CC– Corpus callosum; HPF- Hippocampal formation; LV- Lateral ventricle. **(B) Serological immunoassay of neurofilament light chain** (sNfL) in obese and lean mice. (Ca-c). Comparison of serum NfL levels between lean and obese mice aged 6-months, 1-year, and 2-years; (lean mice, n = 6–18; obese mice, n = 8–18). Technical triplicates were performed for each biological replicate. **(C) RT-PCR quantification of relative expression of BBB proteins, Tight junction protein, Occludin,** in hippocampi and cortices of obese mice. (Da-c) Quantification of expression in hippocampi of 6-months,1-year, and 2-year-old mice. (Dd-f) Quantification of expression in cortices of 6-months (n = 3–6), 1-year-old mice (n = 3–6), and 2-year-old mice (n = 4–6). **(D) RT-PCR quantification of relative expression of BBB proteins, Adherens junction protein, VE-Cadherin,** in hippocampi and cortices of obese mice. (Ea-c) Quantification of expression in hippocampi of 6-months, 1-year, and 2-year-old mice. (Ed-f) Quantification of expression in cortices of 6-months, 1-year, and 2-year-old mice. Lean mice, n = 3–6; obese mice, n = 3–6, for every age group. Technical duplicates were performed for each biological replicate. Welch's *t*-test and one-way ANOVA were applied to the data and represented as mean with SEM.

water-maze test was also performed with 6-months-old cohorts. No significant differences were seen amongst the young cohorts of mice indicating their sound cognitive abilities after the Morris water-maze analysis (Suppl. Fig. 1 d-j).

A comparison of water-maze test performances between 6-months-old and 1-year-old mice was conducted to assess the effect of ageing on cognition in lean and obese mice (Suppl. Fig. 2). Suppl. Fig. 2A shows no difference between the escape latencies of 6-month and 1-year-old lean mice (Suppl. Fig. 2Aa). Suppl. Fig. 2Ab demonstrates that 1-year-old obese mice exhibit significantly higher escape latencies compared to 6-months-old obese mice. Similarly, the cognitive score of lean mice aged 6 months and 1 year are not statistically significantly different (Suppl. Fig. 2Ba). In contrast, the cognitive scores of 1-year-old obese mice are significantly lower compared to 6-months-old obese mice (Suppl. Fig. 2Bb).

3.3. Evidence of neurodegeneration in obese-aged mice with cognitive decline

In order to analyze neurodegeneration, various characteristic hallmarks were tested in the cohorts of obese vs. lean mice. With the analysis of histological sagittal sections of brain, sizes of lateral ventricles of brain were quantified. Fig. 3A(a-c) shows that 1-year-old obese mice brains (n=5) have significantly dilated lateral ventricles as compared to lean mice brains (n=5).

As part of histological analysis, we proceeded to analyze the expression of presynaptic and postsynaptic proteins in brain cryosections using immunofluorescence double-staining. Sagittal brain sections were stained against the presynaptic marker synaptotagmin 1 and the postsynaptic marker PSD95 (Suppl. Fig. 3). We did not observe any significant change in the expression of presynaptic and postsynaptic markers in 1-year-old obese mice. The quantification was performed using Fiji Image J, synapse counter plugin.

Neurofilament light chain (NfL) is a polypeptide biomarker of neuronal damage, and released from axons of damaged neurons. It is usually measured in cerebrospinal fluid (CSF), which is difficult to harvest, to monitor the course of neurodegenerative disorders. Studies (Brenner et al., 2023;100(21):e2204.) have shown that the amount of CSF-NfL corresponded to serum-NfL (sNfL). Fig. 3B shows the serological immunoassay of NfL performed in obese and lean mice using highly sensitive and specific instrument Ella™ (Bio-techne, Minneapolis, USA). Several studies report that body weight is a confounding factor affecting NfL level (Freedman et al., 2024; Rebelos et al., 2022; Manouchehrinia et al., 2020). The sNfL concentrations were measured in both obese and lean mice across all age groups. The levels of sNfL, normalized to the body weight, were increased in obese mice compared to lean mice. Fig. 3B-a shows a dot-plot graph indicating the concentration of sNfL in 6-months-old mice, with no significant difference between obese and lean mice. However, in 1-year-old obese mice, sNfL levels were significantly higher compared to lean mice (Fig. 3B-b), and this difference was even more pronounced in 2-years-old obese mice (Fig. 3B-c).

Our results are in line with the increase of sNfL levels in normal human ageing, and in obesity-accelerated ageing of humans (Kaeser et al., 2021; Khalil et al., 2020). Thereby, a 1-year-old mouse corresponds to a 45-years-old human and a 2-years-old mouse to an 80-years-old human (Wang et al., 2020).

Ageing is a major factor damaging the physiological and molecular integrity of the blood–brain-barrier (BBB) (Hussain et al., 2021). Damage to BBB renders it dysfunctional by allowing passage of toxins and leading to cognitive impairment and neurodegenerative diseases (Hussain et al., 2021). BBB comprises of tight junctions and adherens junctions, which are formed by several interacting proteins (Kadry et al., 2020). We investigated the expression of one protein each from tight and adherens junction i.e., occludin and VE-cadherin, respectively, in hippocampus and cortex of the brain.

As shown in Fig. 3C, mRNA expression was quantified using RT-PCR.

The relative expression of *occludin* was not altered in 6-months-old obese mice, but a significant reduction was observed in the hippocampi of 1-year-old and 2-years-old obese mice (Fig. 3C-b, c). Interestingly, a significant change in the relative expression of *occludin* was detected in the cortex of 2-years-old obese mice (Fig. 3C-f), whereas no significant change was observed in 6-months-old and 1-year-old obese mice (Fig. 3C-d, e).

Similarly, gene expression of *VE-cadherin* was quantified (Fig. 3D a-c). A significant reduction was seen in the hippocampi of 1-year-old obese mice, but no change was observed in the hippocampus of 6-months-old and 2-years-old obese mice. Consistently, no change was found in the relative expression of *VE-cadherin* in the brain cortex across any age group (Fig. 3D-c, d). This trend mirrors the changes observed with *occludin*.

3.4. Serological evidences of increased systemic inflammation due to obese-ageing

Obesity is considered to be a state of low-grade chronic inflammation (Hildebrandt et al., 2023). We therefore studied several chemokines in sera from obese and lean mice. The levels of CCL2, CXCL10, and TNFα were found to be significantly higher in 6-months and 1-years-old obese vs. lean mice (see Fig. 4A-a, c, e, Fig. 4B-a, b, c, e). Whereas IL6 was found to significantly increase in 1-year-old obese mice (Fig. 4A-b). In contrast, SDF-1α serum levels were significantly reduced in 6-months-old obese mice (Fig. 4A-d), but not in 1-year-old obese mice (Fig. 4B-d), Similarly, IFNγ levels in sera (Fig. 4A-f, B-f) of 6-months and 1-year-old mice did not show significant alterations.

3.5. Histological evidence of neuroinflammation in obese-aged cognition impaired mice

To analyze lipid distribution or accumulation in brains of obese-aged vs. lean mice, we stained sagittal sections of cryopreserved brains with Oil Red O. A visibly high lipid accumulation was seen in the white matter of brain *viz.* fiber tracts, corpus callosum, and cerebellar medulla of 1-year-old obese mice as shown in Fig. 5A-b, while Fig. 5A-a represents a healthy 1-year-old lean mouse brain with regular lipid content. Interestingly, the lipid content in the brain of 2-years-old obese mice (Fig. 5A-d) was higher than that of both its lean counterpart (Fig. 5A-c) as well as the 1-year-old obese mice. Strong lipid deposits were observed in telencephalic fiber tracts such as the corpus callosum and in the medulla of the cerebellum. Obese-ageing obviously causes alterations of the lipid homeostasis in the brain of mice.

Next, brain tissues were stained with antibodies against neuronal marker NeuN, and microglia marker CD11b, in order to examine signs of neuroinflammation. Infiltration of CD11b- positive microglia was seen in the cortical layers, hippocampus, thalamus, corpus collosum, and cerebellum of 1-year-old obese mice (Fig. 5B-b), while a moderate staining of resident microglia was seen in the corresponding lean mice (Fig. 5B-a). A quantitative analysis was performed (using analysis application Hybrid cell count with Keyence microscope) based on the CD11b-positive cell count in 6-months-old, 1-year-old, and 2-years-old mice (Fig. 5B-c, d, e). The statistical analyses showed that microglia count was significantly higher in 1-year-old obese mice vs. lean mice.

3.6. Potential candidate biomarkers of neuro-cognitive impairment and neuropathologies

Gene expression profiling of hippocampus was performed to identify potential candidate biomarkers for early diagnosis of neuropathologies. Biomarkers for neuropathological disorders could also be a tool for diagnosis of approaching neurodegenerative diseases that is prevalent in advanced age. Gene expression profile of hippocampi from 1-year-old obese mice was obtained as a result of the illustrated workflow (Fig. 6A). Illumina Hiseq4000 system generated an extensive list of
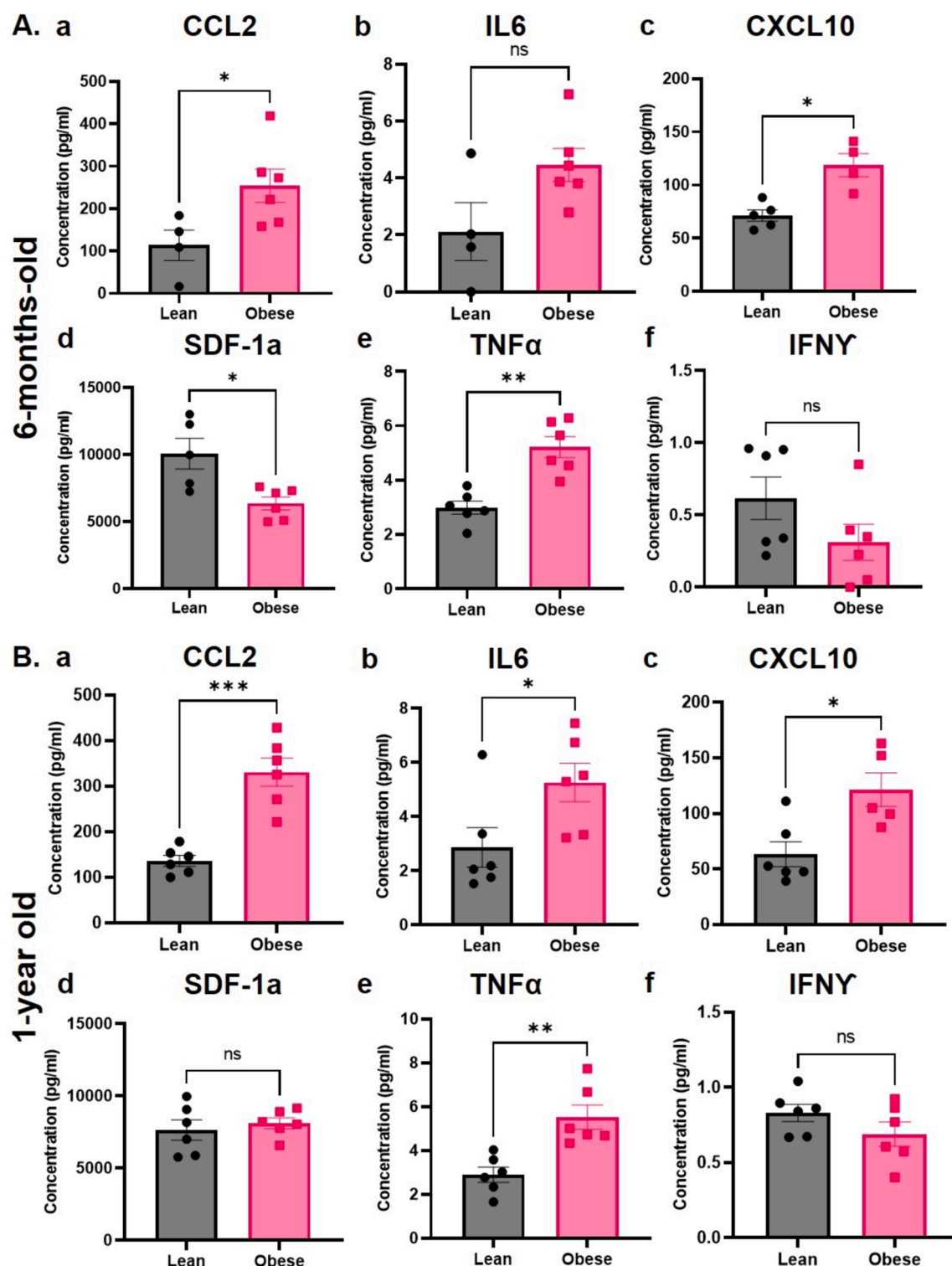
Fig. 4. Serological analysis of systemic inflammation in obese mice. (A) Relative expression of chemokines in the sera of 6-months-old obese vs. lean mice. Chemokines CCL2, IL6, CXCL10, and TNFα were significantly upregulated in obese mice, whereas, SDF-1α was significantly downregulated. INFγ levels in obese mice remained similar to that of the lean mice. (B). Relative expression of chemokines in the sera of 1-year-old obese vs. lean mice. Chemokines CCL2, IL6, CXCL10, TNFα were significantly upregulated in the obese mice, whereas, SDF-1α and INFγ levels in obese mice remained similar to that of the lean mice. One-way ANOVA and Welch's *t*-test were performed to compare lean mice to obese mice and the data is represented as mean with SEM. (Lean, n = 4–6; obese, n = 4–6 for every age group. Technical triplicates were performed for each biological replicate).

significantly differentially expressed genes in obese mice (vs. lean mice) as represented in the heatmap. A gene ontology (GO) overrepresentation analysis was performed with the differentially expressed (DE) genes (upregulated and downregulated) using the clusterProfiler R package (version 4.0.0) (Wu et al., 2021;2(3):100141.). The top 10 significantly enriched pathways from the analysis were selected for visualisation as dot plots. Fig. 6**B-a** (upregulated genes) and **6B-b** (downregulated genes) represent dot plots with significant GO
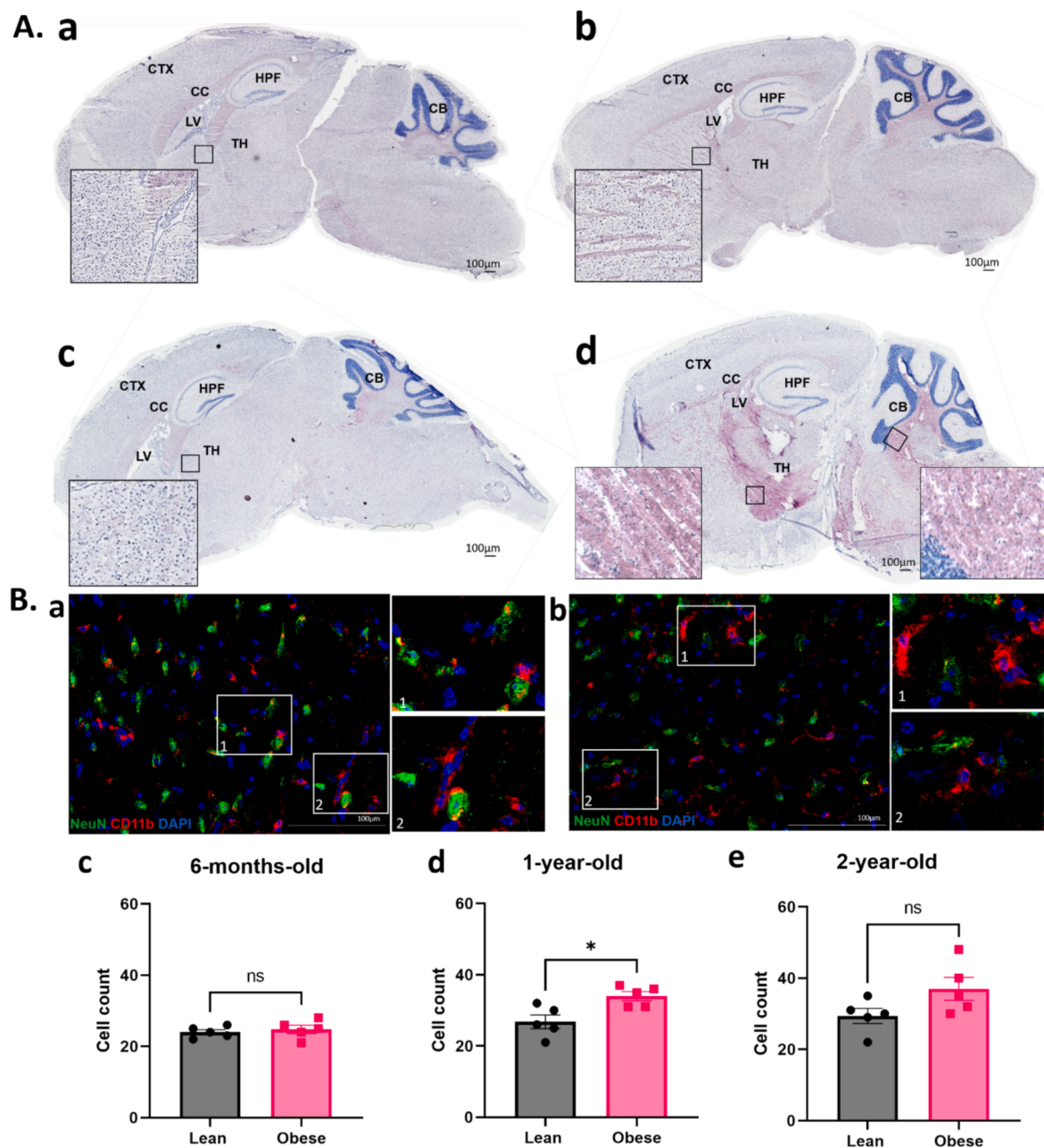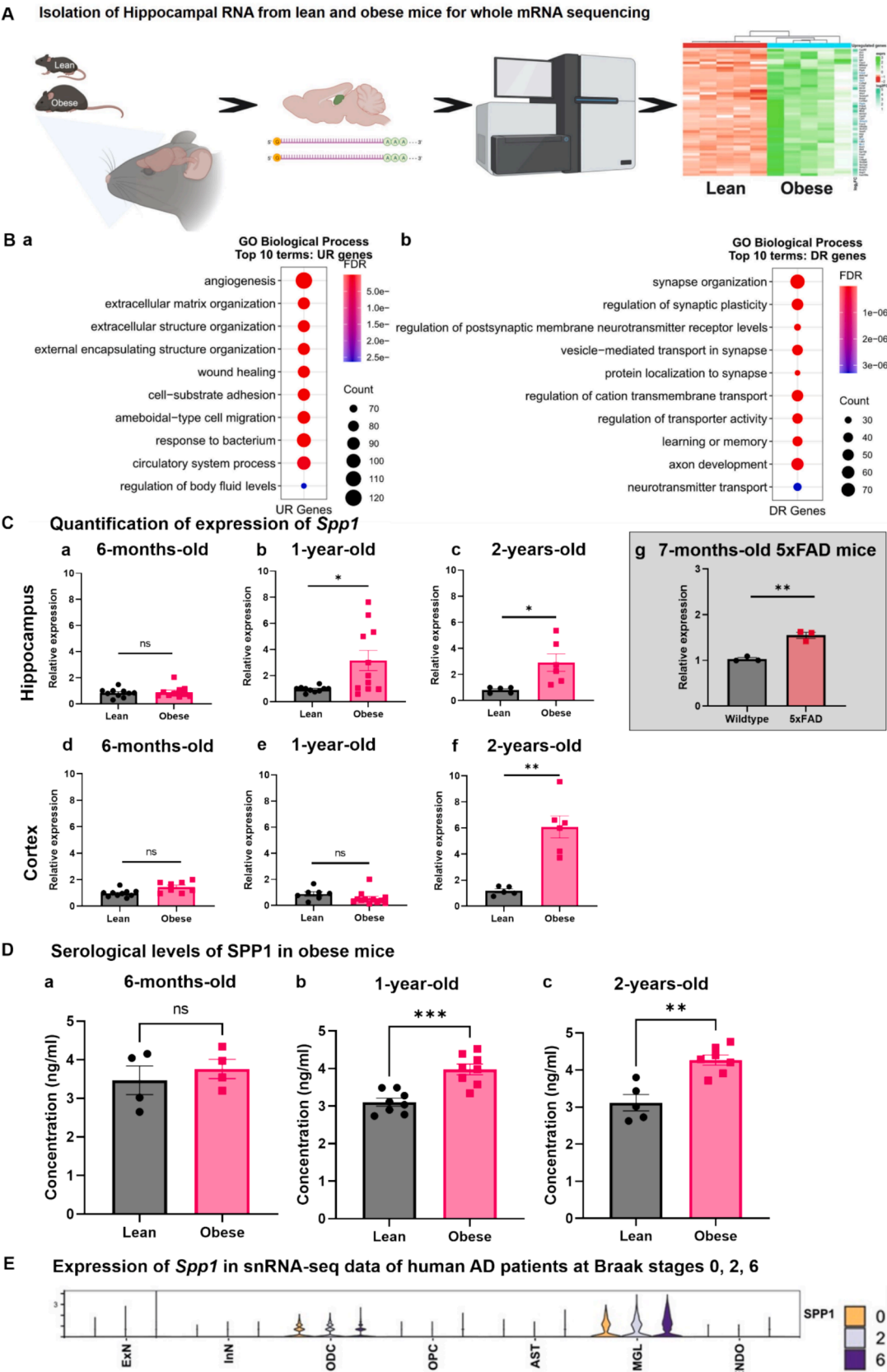
Fig. 5. Influx of lipid is associated with neuroinflammation. (A) Oil Red O-positive regions in the brain of 1-year-old and 2-years-old mice. Representative bright field images showing Oil Red O-positive regions in obese vs. lean mouse brain. (Aa) 1-year-old lean mouse brain. (Ab) 1-year-old obese mouse brain. (Ac) 2-years-old lean mouse brain. (Ad) 2-years-old obese mouse brain. CB- cerebellum; CTX – Cerebral cortex; CC – Corpus callosum; HPF – Hippocampal formation; LV – lateral ventricle; TH – Thalamus. At least 2 sections per brain were analyzed. Scale bar- 100 μm. **(B) Immunofluorescence staining** of brain cryo-sections with antibodies against the neuronal marker **NeuN** and the microglia marker **CD11b** in 1-year-old mice. (Ba) representative image showing microglia from lean mouse brain. (Bb) representative image showing microglia from obese mouse brain. Scale bar- 100 μm. (Bc) **CD11b**-positive microglia cell count in 6-months-old lean and obese mice (lean, n = 5; obese, n = 5). (Bd) CD11b-positive microglia cell count in 1-year-old lean and obese mice (lean, n = 5; obese, n = 5). (Be) CD11b-positive microglia cell count in 2-year-old lean and obese mice (lean, n = 5; obese, n = 5). At least 2 sections per brain were analyzed. One-way ANOVA and Welch's *t*-test were performed to compare cell count in lean mice to obese mice and the data is represented as mean with SEM.

biological processes enriched among the collective list of DE genes. The further screening of regulated genes was done with consideration to role of the genes in brain function and ageing. Using the above-mentioned criterion, we screened secretory phosphoprotein 1 (*Spp1* = osteopontin), hemoglobin beta-s adult chain (*Hbb-bs*), prostaglandin D2 synthase (*Ptgds*), fibromodulin (*Fmod*), and proteoglycan 4 (*Prg4*). Suppl. Fig. 4 shows the quantification of relative expression of candidate genes. Most candidate genes portrayed a significant increase in expression in hippocampi of 1-year and 2-years-old obese mice, however

a variation in relative expression was observed in cortices.

3.6.1. Secretory phosphoprotein 1 a.k.a. Osteopontin

SPP1 is a proinflammatory cytokine that is secreted by active microglial cells in brain (Yu et al., 2017). As a consequence, it is upregulated in brain in case of injury or inflammation and plays a role in neurodegenerative diseases (Riew et al., 2019;16(1):N.PAG-N.PAG.). The transcriptomics data indicated a three-fold upregulation of *Spp1* expression in 1-year-old obese mice hippocampi. Upon verification of

A Isolation of Hippocampal RNA from lean and obese mice for whole mRNA sequencing

B a GO Biological Process Top 10 terms: UR genes

b GO Biological Process Top 10 terms: DR genes

C Quantification of expression of *Spp1*

D Serological levels of SPP1 in obese mice

E Expression of *Spp1* in snRNA-seq data of human AD patients at Braak stages 0, 2, 6

(caption on next page)

Fig. 6. Transcriptomics analysis of hippocampi of Mc4r deficient obese mice. **(A)** Schematic representation of experimental workflow for whole mRNA sequencing of hippocampi samples of 1-year-old mice belonging to lean (n = 5) and obese (n = 5) cohorts. Created with BioRender.com. **(B) Gene Ontology** analysis of differentially expressed genes. (a) Dot plot showing GO biological processes significantly enriched among the upregulated genes. (b) Dot plot showing GO biological processes significantly enriched among the downregulated genes. **(C) Quantitative verification of expression of Spp1**, a potential biomarker of neuropathological disorder and brain dysfunction in hippocampi and cortices of Mc4r-deficient obese mice. (a-c) Relative expression of **Spp1** in the **hippocampi** with progression of age (6-months, 1-year, 2-years) in obese mice. (d-f). Relative expression of **Spp1** in the **cortices** with progression of age (6-months, 1-year, 2-years) in obese mice. Lean mice (n = 5–10) and obese mice (n = 6–12) for each age group. (g) Relative expression of **Spp1** in the **hippocampi** of 7-month-old 5xFAD mice compared to WT mice. 5xFAD mice (n = 3) and WT mice (n = 3). Mean with SEM are shown. **(D) Serological ELISA of SPP1 in obese and lean mice.** (a) Graphical representation of serum SPP1 levels in lean and obese mice aged 6-months, (b) aged 1-year and (c) aged 2-years. Welch's *t*-test and one-way ANOVA were performed to compare lean mice to obese mice and the data is represented as mean with SEM. (Lean, n = 4–8; obese, n = 4–8). Technical duplicates were performed for each biological replicate. **(E).** Spp1 expression in **snRNA-Seq** of postmortem brain of AD patients at braak stage 0, 2, and 6. ExN- Excitatory neurons, InN- Inhibitory neurons, ODC- oligodendrocytes, OPC- oligodendrocyte precursor cells, AST- astrocytes, MGL- microglia, ENDO- endothelial cells.

Spp1 using qPCR, it was verified that *Spp1* has a significant three-fold upregulation of expression in the hippocampi of 1-year and 2-years-old obese mice (Fig. 6**C**). Additionally, it showed an almost six-fold higher expression in cortices of 2-years-old obese mice, which was highly significant (Fig. 6**C-f**).

To test the reliability of *Spp1* as a potential marker for neurodegeneration in an Alzheimer disease model, its expression was also quantified in the hippocampi of 7-months-old 5xFAD mice (n=3), which overexpress mutated human APP and PSEN1 (Oakley et al., 2006), against healthy lean mice (n=3). A significant increase in *Spp1* expression was seen in the 5xFAD mice (Fig. 6**C-g**).

To address the question, whether Spp1 could serve as a potential biomarker we analyzed blood level. SPP1/osteopontin has two subtypes −secreted and intracellular (Cantor and Shinohara, 2009). Secreted SPP1 was tested in mice sera (6-months, 1-year, and 2-years-old) using conventional ELISA. The known standard absorbance values were plotted into a standard curve by using sigmoid function. The sigmoid standard curve was then used to interpolate SPP1 content in mice sera. Fig. 6**D** exhibits the SPP1 levels in lean and obese mice sera. 6-months-old obese mice showed insignificant difference as compared to corresponding lean litter mates (Fig. 6**D-a**). 1-year-old obese mice showed a highly significant increase in the serological levels of SPP1, which was also seen in 2-years-old obese mice (Fig. 6**D-b, c**).

Potency of Spp1 as a diagnostic marker was further validated by checking the expression profile of *Spp1* in a publicly available single-nucleus RNA sequencing (snRNA-Seq) data-set (Leng et al., 2021). The snRNA-Seq was performed on cell nuclei from postmortem brain tissue (superior frontal gyrus and entorhinal cortex) from AD patients at different braak stages (0, 2, and 6). Post analysis, it was found that *Spp1* is selectively expressed in oligodendrocytes and microglial cells from the superior frontal gyrus data-set. Interestingly, the *Spp1* expression was found to increase from braak stage 0 to 6 in AD patients (Fig. 6**E**).

4. Discussion

Obesity and ageing are major contributors to a number of diseases that can limit life expectancy, and both conditions have common or overlapping mechanisms. Therefore, we investigated the role of obese-ageing in a well-established mouse model, specifically C57BL/6J loxTB Mc4r knock-out mice. As shown previously, homozygous *Mc4r* knock-out mice become massively obese due to the lack of satiety (Balthasar et al., 0000). Here, we studied the mice for more than 2 years. Of note, we have observed the same life expectancy as their lean litter mates.

We aimed to understand how obesity influences the brain and accelerates ageing processes. Therefore, we chose a model of obesity using *Mc4r* knock-out mice. The *Mc4r* knock-out mouse model, known for obesity and a proinflammatory phenotype, was chosen given the well-accepted link between MC4R loss in humans and obesity (Farooqi et al., 0000). *Mc4r* knock-out mice lack the sense of satiety and develop obesity with a proinflammatory phenotype by the age of 6 months (Itoh et al., 2011). In addition, there is indirect evidence that *Mc4r* may play a role in mitigating cognitive dysfunction. Activation of melanocortin

receptors with agonists has shown to improve amyloid pathology in a human-adapted mouse model of AD (APP/PS1 mouse) by reducing inflammation in the brain (Jackie et al., 2021). It is assumed that a 1-year-old mouse corresponds to a 45-years-old human and a 2-years-old mouse to an 80-years-old human (Wang et al., 2020). The *Mc4r* knock-out mouse model may therefore help investigating the effects of obesity on age-related neurodegenerative diseases.

We employed a rigorous scientific approach, including the use of a well-established mouse model (*Mc4r* knock-out mice) and various analytical techniques such as behavioral tests, RNA-Seq, and histological analyses to investigate the impact of obesity on ageing and neurodegenerative diseases.

Histological analyses revealed a high lipid content along with increased microglial cell count in the brain of obese mice as compared to the lean mice. Transcriptional analyses identified a number of genes potentially linked to obesity-related cognitive decline and neuroinflammation. Our study proposes Spp1 as a promising candidate for early neurodegenerative disease diagnosis based on analyses of serum proinflammatory markers.

Overall, the study provides novel insights into the complex relationship between obesity, ageing, and neurodegenerative diseases, using a comprehensive approach involving genetic, histological, and biochemical analyses in a relevant mouse model.

4.1. Obese-ageing affects cognition

We used the *Mc4r* knock-out mouse model to study potential correlations between BMI, ageing, and cognitive decline. There are now a large number of studies that show that it is possible to study cognitive functions in mice (Tanila, 2018; Niu et al., 2022). A wide range of behavioral tests are available for laboratory rodents to analyze complex behaviors related to cognition. The cognitive component is reflected by the ability to acquire relevant information during learning processes. Thereby, the hippocampus is the main organ responsible for learning and memory (Hou et al., 2019).

Our data show that *Mc4r*-deficient-mice gain significant weight and become severely obese by the age of 6 month. After that, their weight remains stable and even reduces to some extent at the age of 2 years. However, they remain significantly heavier than the wildtype litter mates.

The mice younger than 6 months were not included in the experimental design because the mice at the age of 6 month did not show any significant neurodegenerative changes; therefore, served as the baseline for the 1-year-old and 2-years-old mice. In the same line, 2-years-old mice were also excluded, as they reportedly display advanced age-related changes (Kerr et al., 2024; Zumerle et al., 2024) that could confound the effects observed in the study.

Based on literature and our own observation, the primary focus was directed on 1-year-old mice, since they are considered middle-aged and exhibit early signs of neurodegeneration that are appropriate for studying disease mechanisms.

Using open-field and water-maze tests, we were able to detect cognitive impairment in the obese *Mc4r*-null mice, similar to a previous

investigation in which obesity was induced by high-fat diet (HFD) to 2-months-old mice for 7 weeks. (Buie et al., 0000, Yoshizaki et al., 0000).

It is noteworthy that despite increased body weight, obese mice do not exhibit locomotor issues, with body weights not differing significantly between 6-months-old and 1-year-old obese mice, while cognitive decline was evident in the 1-year-old obese mice. In contrast, the time required to complete the task (escape latency) and the subsequent cognitive scores differed significantly between these age groups (suppl. Fig. 2). Our data indicates that obesity leads to cognitive impairment in mice that is exacerbated with age, starting in 1-year-old mice.

A plausible explanation for the memory impairment and cognitive functions could be activated endoplasmic reticulum stress, as indicated in a mouse model of HFD-induced obesity (Niu et al., 2022). In addition, both obesity and ageing lead to dysfunction of nitric oxide signaling, which impairs blood flow to the brain, and decreases synaptic plasticity in the hippocampus (Buie et al., 0000), which negatively affects cognitive abilities. Together, previous reports and our data clearly indicate that obesity leads to cognitive impairment that worsens with age.

The study connects findings from an obese-ageing mouse model to potential implications for human health. The choice of the *Mc4r* knock-out mouse model, a known model for obesity and lack of satiety, provides a relevant context for understanding the potential effects of obesity on age-related neurodegenerative diseases in humans.

4.2. Neuroinflammation

In addition to cognitive decline, neuroinflammation is an early manifestation of neurodegenerative diseases. There are reports describing the mechanisms by which obesity triggers both cognitive decline and inflammation. The most widely accepted mechanism is that obesity triggers both systemic and central nervous system inflammation. Similarly, the accumulation of lipids in the brain can trigger local inflammation through the activation of microglial cells. Microglial cells are the immune cells of the CNS with phagocytic function important for removing harmful substances that may cause inflammation (Yang et al., 2010). This step is crucial for the termination of inflammation because long-term inflammation and sustained release of proinflammatory cytokines from adipose or local tissues leads to organ damage, resulting in suppression of neuronal and cognitive functions (Frasca et al., 2017; Leng and Edison, 2021; Yang et al., 2010). Our findings are in line with these observations. We observed both local and systemic inflammation in obese *Mc4r* knock-out mice subsequent to fat accumulation in the brain and accumulation of microglial cells together with markers for neurodegeneration. Indeed, previous studies have demonstrated a link between neurodegenerative diseases and lipid deposition in the brain (Farmer et al., 2020).

The notion of obesity-induced inflammation is supported by the fact that in the hippocampus of the *Mc4r* knock-out mice, there is an alteration in the expression of tight and adherens junction genes (*occludin* and *VE-cadherin*) responsible for blood–brain barrier (BBB) integrity (Tunggal et al., 0000; Li et al., 2018), suggesting leakiness of the barrier.

Another striking observation of the study was that the levels of pro-inflammatory mediators continued to increase with age, interestingly, a significant increase in the body weight of the obese mice compared to lean mice was also observed in all groups studied. This may suggest that either obesity and/or ageing are the main driver of this process, which could trigger pro-inflammatory pathways.

There have been some evidences that the cognitive decline and neuroinflammation observed in the *Mc4r* knock-out mice are primarily due to obesity and not due to the knockout of the *Mc4r* gene itself or ageing.

Indeed, the metabolic syndrome that often accompanies obesity, including chronic systemic inflammation and dyslipidemia, can have profound effects on brain function. These effects are likely exacerbated in *Mc4r* knock-out mice due to the severe obesity they develop. In addition, our data suggest that obesity triggers a state of chronic low-grade inflammation, including in the brain (Tam et al., 2020; Frasca et al., 2017). This inflammation is associated with the activation of microglial cells, which leads to neurodegenerative changes that are a key factor in cognitive decline.

Next, in search of potential candidates that could serve as a biomarker(s) for the detection of obesity-related neuroinflammation and cognitive decline, which are early signs of NDD. We carried out RNA-Seq analyses, which revealed an extensive list of differentially expressed genes that could be potential targets for diagnosis or treatment of brain inflammation and cognitive decline. Among them, *Spp1* emerged as the most prominent candidate in our study due to its elevated levels at mRNA in addition to protein levels in serum, making it an attractive and testable candidate biomarker in human blood. Several studies have reported that Spp1 plays an important role in neuroinflammation in several neurodegenerative disorders (de Luna et al., 2023; Al-Dalahmah et al., 2024), moreover, a recent study shows its association with cognitive decline has now been documented in humans (de Lopes et al., 2024).

In our study, cognitive decline, elevated numbers of activated microglia, and increased neuro- and systemic inflammation were positively correlated with *Spp1* levels in brain tissue and serum of 1-year-old obese mice.

This suggests that SSP1 may serve as a potential blood biomarker for the early diagnosis of cognitive decline, though BMI should be taken into account when interpreting SPP1 levels.

5. Conclusions

Our data show that loss-of-*Mc4r*-induced hyperphagia is associated with obesity-related cognitive decline and neuroinflammation accelerated by ageing. In addition, our transcriptional data revealed a number of genes potentially involved in obesity-related cognitive decline and neuroinflammation. We identified SPP1 as a novel and most prominent marker, which appears to be an early diagnostic marker and probably a trigger of cognitive decline and neuroinflammation. This has practical implications for the field, as early diagnosis is crucial for effective intervention and treatment. We conclude that obesity and ageing share several mechanisms that increase the likelihood of neurodegenerative diseases.

CRediT authorship contribution statement

Mansi Rajput: Writing – original draft, Visualization, Validation, Investigation, Formal analysis. **Ihtzaz Ahmed Malik:** Writing – original draft, Supervision, Investigation, Conceptualization. **Aditi Methi:** Formal analysis. **Jonathan Alexis Cortés Silva:** Formal analysis. **Dorothea Fey:** Investigation. **Oliver Wirths:** Writing – review & editing. **André Fischer:** Supervision, Resources. **Jörg Wilting:** Writing – review & editing. **Christine A.F. von Arnim:** Writing – review & editing, Resources, Funding acquisition.

Declaration of competing interest

Appendix A. Supplementary data

Supplementary data to this article can be found online at https://doi. org/10.1016/j.bbi.2024.12.154.

Data availability

Data will be made available on request.

References

Agrawal M. Chapter 26 - Molecular basis of chronic neurodegeneration. In: Kumar D, ed. *Clinical Molecular Medicine.* Academic Press; 2020:447-460. doi:10.1016/B978-0-12-809356-6.00026-5.

Albanese, E., Launer, L.J., Egger, M., et al., 2017. Body mass index in midlife and dementia: Systematic review and meta-regression analysis of 589,649 men and women followed in longitudinal studies. *Alzheimers Dement Amst Neth.* 8, 165–178. https://doi.org/10.1016/j.dadm.2017.05.007.

Al-Dalahmah, O., Lam, M., McInvale, J.J., et al., 2024. Osteopontin drives neuroinflammation and cell loss in MAPT-N279K frontotemporal dementia patient neurons. *Cell Stem Cell.* 31 (5), 676–693.e10. https://doi.org/10.1016/j. stem.2024.03.013.

Balthasar N, Dalgaard L, Lee C, et al. Divergence of melanocortin pathways in the control of food intake and energy expenditure. Cell. doi:10.1016/j.cell.2005.08.035.

Brenner, J., Mariotto, S., Bastiaansen, A.E.M., et al., 2023;100(21):e2204.. Predictive Value of Serum Neurofilament Light Chain Levels in Anti-NMDA Receptor Encephalitis. *Neurology.* https://doi.org/10.1212/WNL.0000000000207221.

Brown, R.C., Lockwood, A.H., Sonawane, B.R., 2005. Neurodegenerative Diseases: An Overview of Environmental Risk Factors. *Environ Health Perspect.* 113 (9), 1250–1256. https://doi.org/10.1289/ehp.7567.

Buie J, Watson L, Smith C, Sims-Robinson C. Obesity-related cognitive impairment: The role of endothelial dysfunction. Neurobiology of disease. doi:10.1016/j. nbd.2019.104580.

Cantor, H., Shinohara, M.L., 2009. Regulation of T-helper-cell lineage development by osteopontin: the inside story. *Nat Rev Immunol.* 9 (2), 137–141. https://doi.org/10.1038/nri2460.

Chen, W., Zhang, X., Huang, W., 2016. Role of neuroinflammation in neurodegenerative diseases (Review). *Mol Med Rep.* 13 (4), 3391–3396. https://doi.org/10.3892/mmr.2016.4948.

Culpan, D., MacGowan, S.H., Ford, J.M., et al., 2003. Tumour necrosis factor-alpha gene polymorphisms and Alzheimer's disease. *Neurosci Lett.* 350 (1), 61–65. https://doi.org/10.1016/s0304-3940(03)00854-1.

de Lopes, K.P., Yu, L., Shen, X., et al., 2024. Associations of cortical SPP1 and ITGAX with cognition and common neuropathologies in older adults. *Alzheimers Dement.*. 20 (1), 525–537. https://doi.org/10.1002/alz.13474.

de Luna, N., Carbayo, Á., Dols-Icardo, O., et al., 2023. Neuroinflammation-Related Proteins NOD2 and Spp1 Are Abnormally Upregulated in Amyotrophic Lateral Sclerosis. *Neurol Neuroimmunol Neuroinflammation.* 10 (2), e200072. https://doi.org/10.1212/NXI.0000000000200072.

Elena, S.G., Surbhi, S., Robin, M.D., Sze-Yen, T., 2022. Is there an association between non-alcoholic fatty liver disease and cognitive function? A Systematic Review. *BMC Geriatr.* 22, 47.

Engelhart, M.J., Geerlings, M.I., Meijer, J., et al., 2004. Inflammatory proteins in plasma and the risk of dementia: the rotterdam study. *Arch Neurol.* 61 (5), 668–672. https://doi.org/10.1001/archneur.61.5.668.

Farmer, B.C., Walsh, A.E., Kluemper, J.C., Johnson, L.A., 2020. Lipid Droplets in Neurodegenerative Disorders. *Front Neurosci.* 14, 547841. https://doi.org/10.3389/fnins.2020.00742.

Farooqi S, Keogh JM, Yeo GSH, Lank EJ, Cheetham T, O'Rahilly S. Clinical spectrum of obesity and mutations in the melanocortin 4 receptor gene. The New England journal of medicine. doi:10.1056/NEJMoa022050.

Frasca, D., Blomberg, B.B., Paganelli, R., 2017. Aging, Obesity, and Inflammatory Age-Related Diseases. *Front Immunol.* 8. https://doi.org/10.3389/fimmu.2017.01745.

Freedman MS, Gnanapavan S, Booth RA, et al. Guidance for use of neurofilament light chain as a cerebrospinal fluid and blood biomarker in multiple sclerosis management. *eBioMedicine.* 2024;101:104970. doi:10.1016/j.ebiom.2024.104970.

Gonzales, M.M., Garbarino, V.R., Pollet, E., et al., 2022. Biological aging processes underlying cognitive decline and neurodegenerative disease. *J Clin Invest.* 132 (10). https://doi.org/10.1172/JCI158453.

Hildebrandt, X., Ibrahim, M., Peltzer, N., 2023. Cell death and inflammation during obesity: "Know my methods, WAT(son). *Cell Death Differ.* 30 (2), 279–292. https://doi.org/10.1038/s41418-022-01062-4.

Hong, S., Beja-Glasser, V.F., Nfonoyim, B.M., et al., 2016. Complement and microglia mediate early synapse loss in Alzheimer mouse models. *Science.* 352 (6286), 712–716. https://doi.org/10.1126/science.aad8373.

Hou, Y., Dan, X., Babbar, M., et al., 2019. Ageing as a risk factor for neurodegenerative disease. *Nat Rev Neurol.* 15 (10), 565–581. https://doi.org/10.1038/s41582-019-0244-7.

Hussain, B., Fang, C., Chang, J., 2021. Blood–Brain Barrier Breakdown: An Emerging Biomarker of Cognitive Impairment in Normal Aging and Dementia. *Front Neurosci.* 15. https://doi.org/10.3389/fnins.2021.688090.

Huszar D, Lynch C, Fairchild-Huntress V, et al. Targeted disruption of the melanocortin-4 receptor results in obesity in mice. Cell. doi:10.1016/s0092-8674(00)81865-6.

Illouz, T., Madar, R., Louzon, Y., Griffioen, K.J., Okun, E., 2016. Unraveling cognitive traits using the Morris water maze unbiased strategy classification (MUST-C) algorithm. *Brain Behav Immun.* 52, 132–144. https://doi.org/10.1016/j.bbi.2015.10.013.

Islam, M.R., Kaurani, L., Berulava, T., et al., 2021. A microRNA signature that correlates with cognition and is a target against cognitive decline. *EMBO Mol Med.* 13 (11), e13659. https://doi.org/10.15252/emmm.202013659.

Itoh, M., Suganami, T., Nakagawa, N., et al., 2011. Melanocortin 4 Receptor–Deficient Mice as a Novel Mouse Model of Nonalcoholic Steatohepatitis. *Am J Pathol.* 179 (5), 2454–2463. https://doi.org/10.1016/j.ajpath.2011.07.014.

Jackie, K.Y.L., Min, T., Yang, S., et al., 2021. Melanocortin receptor activation alleviates amyloid pathology and glial reactivity in an Alzheimer's disease transgenic mouse model. *Sci Rep.* 11 (1), 1–15. https://doi.org/10.1038/s41598-021-83932-4.

Jonsson, T., Stefansson, H., Steinberg, S., et al., 2013. Variant of TREM2 associated with the risk of Alzheimer's disease. *N Engl J Med.* 368 (2), 107–116. https://doi.org/10.1056/NEJMoa1211103.

Kadry, H., Noorani, B., Cucullo, L., 2020. A blood–brain barrier overview on structure, function, impairment, and biomarkers of integrity. *Fluids Barriers CNS.* 17 (1), 69. https://doi.org/10.1186/s12987-020-00230-3.

Kaeser, S.A., Lehallier, B., Thinggaard, M., et al., 2021. A neuronal blood marker is associated with mortality in old age. *Nat Aging.* 1 (2), 218–225. https://doi.org/10.1038/s43587-021-00028-4.

Kerr, H.L., Krumm, K., Anderson, B., et al., 2024. Mouse sarcopenia model reveals sex- and age-specific differences in phenotypic and molecular characteristics. *J Clin Invest.* 134 (16). https://doi.org/10.1172/JCI172890.

Khalil, M., Pirpamer, L., Hofer, E., et al., 2020. Serum neurofilament light levels in normal aging and their association with morphologic brain changes. *Nat Commun.* 11 (1), 812. https://doi.org/10.1038/s41467-020-14612-6.

Kishi, T., Aschkenasi, C.J., Lee, C.E., Mountjoy, K.G., Saper, C.B., Elmquist, J.K., 2003. Expression of melanocortin 4 receptor mRNA in the central nervous system of the rat. *J Comp Neurol.* 457 (3), 213–235. https://doi.org/10.1002/cne.10454.

Leng, F., Edison, P., 2021. Neuroinflammation and microglial activation in Alzheimer disease: where do we go from here? *Nat Rev Neurol.* 17 (3), 157–172. https://doi.org/10.1038/s41582-020-00435-y.

Leng, K., Li, E., Eser, R., et al., 2021. Molecular characterization of selectively vulnerable neurons in Alzheimer's disease. *Nat Neurosci.* 24 (2), 276–287. https://doi.org/10.1038/s41593-020-00764-7.

Li, W., Chen, Z., Chin, I., Chen, Z., Dai, H., 2018. The Role of VE-cadherin in Blood-brain Barrier Integrity under Central Nervous System Pathological Conditions. *Curr Neuropharmacol.* 16 (9), 1375–1384. https://doi.org/10.2174/1570159X16666180222164809.

Livak, K.J., Schmittgen, T.D., 2001. Analysis of Relative Gene Expression Data Using Real-Time Quantitative PCR and the $2^{-\Delta\Delta CT}$ Method. *Methods.* 25 (4), 402–408. https://doi.org/10.1006/meth.2001.1262.

Malik, I.A., Triebel, J., Posselt, J., et al., 2012. Melanocortin receptors in rat liver cells: change of gene expression and intracellular localization during acute-phase response. *Histochem Cell Biol.* 137 (3), 279–291. https://doi.org/10.1007/s00418-011-0899-7.

Manouchehrinia, A., Piehl, F., Hillert, J., et al., 2020. Confounding effect of blood volume and body mass index on blood neurofilament light chain levels. *Ann Clin Transl Neurol.* 7 (1), 139–143. https://doi.org/10.1002/acn3.50972.

Morris, R., 1984. Developments of a water-maze procedure for studying spatial learning in the rat. *J Neurosci Methods.* 11 (1), 47–60. https://doi.org/10.1016/0165-0270(84)90007-4.

Morys, F., Potvin, O., Zeighami, Y., et al., 2023. Obesity-Associated Neurodegeneration Pattern Mimics Alzheimer's Disease in an Observational Cohort Study. *J Alzheimers Dis.* 91 (3), 1059–1071. https://doi.org/10.3233/JAD-220535.

Namjou, B., Stanaway, I.B., Lingren, T., et al., 2021. Evaluation of the MC4R gene across eMERGE network identifies many unreported obesity-associated variants. *Int J Obes.* 45 (1), 155–169. https://doi.org/10.1038/s41366-020-00675-4.

Niu, Y., Chang, P., Liu, T., et al., 2022. Obese mice induced by high-fat diet have differential expression of circular RNAs involved in endoplasmic reticulum stress and neuronal synaptic plasticity of hippocampus leading to obesity-associated cognitive impairment. *Front Mol Neurosci.* 15, 1000482. https://doi.org/10.3389/fnmol.2022.1000482.

Oakley, H., Cole, S.L., Logan, S., et al., 2006. Intraneuronal β-Amyloid Aggregates, Neurodegeneration, and Neuron Loss in Transgenic Mice with Five Familial Alzheimer's Disease Mutations: Potential Factors in Amyloid Plaque Formation. *J Neurosci*. 26 (40), 10129. https://doi.org/10.1523/JNEUROSCI.1202-06.2006.

Perry, V.H., Cunningham, C., Holmes, C., 2007. Systemic infections and inflammation affect chronic neurodegeneration. *Nat Rev Immunol*. 7 (2), 161–167. https://doi.org/10.1038/nri2015.

Rebelos, E., Rissanen, E., Bucci, M., et al., 2022. Circulating neurofilament is linked with morbid obesity, renal function, and brain density. *Sci Rep*. 12 (1), 7841. https://doi.org/10.1038/s41598-022-11557-2.

Redman, L.M., Smith, S.R., Burton, J.H., Martin, C.K., Il'yasova, D., Ravussin, E., 2018. Metabolic Slowing and Reduced Oxidative Damage with Sustained Caloric Restriction Supports the Rate of Living and Oxidative Damage Theories of Aging. *Cell Metab*. 27 (4), 805–815.e4. https://doi.org/10.1016/j.cmet.2018.02.019.

Riew, T.R., Kim, S., Jin, X., Kim, H.L., Lee, J.H., Lee, M.Y., 2019;16(1):N.PAG-N.PAG.. Osteopontin and its spatiotemporal relationship with glial cells in the striatum of rats treated with mitochondrial toxin 3-nitropropionic acid: possible involvement in phagocytosis. *J Neuroinflammation*. https://doi.org/10.1186/s12974-019-1489-1.

Scheltens, P., Blennow, K., Breteler, M.M.B., et al., 2016. Alzheimer's disease. *Lancet Lond Engl*. 388 (10043), 505–517. https://doi.org/10.1016/S0140-6736(15)01124-1.

Tam, B.T., Morais, J.A., Santosa, S., 2020. Obesity and ageing: Two sides of the same coin. *Obes Rev off J Int Assoc Study Obes*. 21 (4), e12991. https://doi.org/10.1111/obr.12991.

Tanila, H., 2018. Testing cognitive functions in rodent disease models: Present pitfalls and future perspectives. *Behav Brain Res*. 352, 23–27. https://doi.org/10.1016/j.bbr.2017.05.040.

Tao, Y.X., 2010. The Melanocortin-4 Receptor: Physiology, Pharmacology, and Pathophysiology. *Endocr Rev*. 31 (4), 506–543. https://doi.org/10.1210/er.2009-0037.

Tunggal J, Helfrich I, Schmitz A, et al. E-cadherin is essential for in vivo epidermal barrier function by regulating tight junctions. The EMBO journal. doi:10.1038/sj.emboj.7600605.

Wang, S., Lai, X., Deng, Y., Song, Y., 2020. Correlation between mouse age and human age in anti-tumor research: Significance and method establishment. *Life Sci*. 242, 117242. https://doi.org/10.1016/j.lfs.2019.117242.

Wu, T., Hu, E., Xu, S., et al., 2021. clusterProfiler 4.0: A universal enrichment tool for interpreting omics data. *The Innovation*. 2 (3), 100141. https://doi.org/10.1016/j.xinn.2021.100141.

Yang, I., Han, S.J., Kaur, G., Crane, C., Parsa, A.T., 2010. The Role of Microglia in Central Nervous System Immunity and Glioma Immunology. *J Clin Neurosci off J Neurosurg Soc Australas*. 17 (1), 6–10. https://doi.org/10.1016/j.jocn.2009.05.006.

Yeo, G.S.H., Lank, E.J., Farooqi, I.S., Keogh, J., Challis, B.G., O'Rahilly, S., 2003. Mutations in the human melanocortin-4 receptor gene associated with severe familial obesity disrupts receptor function through multiple molecular mechanisms. *Hum Mol Genet*. 12 (5), 561–574. https://doi.org/10.1093/hmg/ddg057.

Yoshizaki K, Asai M, Hara T. High-Fat Diet Enhances Working Memory in the Y-Maze Test in Male C57BL/6J Mice with Less Anxiety in the Elevated Plus Maze Test. Nutrients. doi:10.3390/nu12072036.

Yu H, Liu X, Zhong Y. The Effect of Osteopontin on Microglia. Malm T, ed. *BioMed Res Int*. 2017;2017:1879437. doi:10.1155/2017/1879437.

Zhou, Y., Chawla, M.K., Rios-Monterrosa, J.L., et al., 2021. Aged brains express less melanocortin receptors, which correlates with age-related decline of cognitive functions. *Molecules*. 26 (20). https://doi.org/10.3390/molecules26206266.

Zumerle, S., Sarill, M., Saponaro, M., et al., 2024. Targeting senescence induced by age or chemotherapy with a polyphenol-rich natural extract improves longevity and healthspan in mice. *Nat Aging*. 4 (9), 1231–1248. https://doi.org/10.1038/s43587-024-00663-7.